

This is a repository copy of *The influence of seawater pCO<sub>2</sub> and temperature on the amino acid composition and aragonite CO<sub>3</sub> disorder of coral skeletons.*

White Rose Research Online URL for this paper:

<https://eprints.whiterose.ac.uk/215926/>

Version: Published Version

---

**Article:**

Allison, Nicola, Ross, Phoebe, Castillo Alvarez, Cristina et al. (9 more authors) (2024) The influence of seawater pCO<sub>2</sub> and temperature on the amino acid composition and aragonite CO<sub>3</sub> disorder of coral skeletons. *Coral reefs*. ISSN 0722-4028

<https://doi.org/10.1007/s00338-024-02539-z>

---

**Reuse**

This article is distributed under the terms of the Creative Commons Attribution (CC BY) licence. This licence allows you to distribute, remix, tweak, and build upon the work, even commercially, as long as you credit the authors for the original work. More information and the full terms of the licence here:

<https://creativecommons.org/licenses/>

**Takedown**

If you consider content in White Rose Research Online to be in breach of UK law, please notify us by emailing [eprints@whiterose.ac.uk](mailto:eprints@whiterose.ac.uk) including the URL of the record and the reason for the withdrawal request.



# The influence of seawater pCO<sub>2</sub> and temperature on the amino acid composition and aragonite CO<sub>3</sub> disorder of coral skeletons

Nicola Allison<sup>1,2</sup> · Phoebe Ross<sup>1</sup> · Cristina Castillo Alvarez<sup>1,2</sup> · Kirsty Penkman<sup>3</sup> · Roland Kröger<sup>4</sup> · Celeste Kellock<sup>1</sup> · Catherine Cole<sup>1</sup> · Matthieu Clog<sup>5</sup> · David Evans<sup>1,8</sup> · Chris Hintz<sup>6</sup> · Ken Hintz<sup>7,9</sup> · Adrian A. Finch<sup>1</sup>

Received: 4 March 2024 / Accepted: 1 August 2024  
© The Author(s) 2024

**Abstract** Coral skeletons are composites of aragonite and biomolecules. We report the concentrations of 11 amino acids in massive *Porites* spp. coral skeletons cultured at two temperatures (25 °C and 28 °C) and 3 seawater pCO<sub>2</sub> (180, 400 and 750 μatm). Coral skeletal aspartic acid/asparagine (Asx), glutamic acid/glutamine (Glx), glycine, serine and total amino acid concentrations are significantly higher at 28 °C than at 25 °C. Skeletal Asx, Glx, Gly, Ser, Ala, L-Thr and total amino acid are significantly lower at 180 μatm seawater pCO<sub>2</sub> compared to 400 μatm, and Ser is reduced at 180 μatm compared to 750 μatm. Concentrations of all skeletal amino acids are significantly inversely related to

coral calcification rate but not to calcification media pH. Raman spectroscopy of these and additional specimens indicates that CO<sub>3</sub> disorder in the skeletal aragonite lattice is not affected by seawater pCO<sub>2</sub> but decreases at the higher temperature. This is contrary to observations in synthetic aragonite where disorder is positively related to the aragonite precipitation rate mediated by either increasing temperature (this study) or increasing Ω (this study and a previous report) and to the concentration of amino acid in the precipitation media (a previous report). We observe no significant relationship between structural disorder and coral calcification rate or skeletal [amino acid]. Both temperature and seawater pCO<sub>2</sub> can significantly affect skeletal amino acid composition, and further work is required to clarify how environmental change mediates disorder.

**Supplementary Information** The online version contains supplementary material available at <https://doi.org/10.1007/s00338-024-02539-z>.

✉ Nicola Allison  
na9@st-andrews.ac.uk

<sup>1</sup> School of Earth and Environmental Sciences, University of St. Andrews, St. Andrews KY16 9TS, UK

<sup>2</sup> Scottish Oceans Institute, University of St. Andrews, St. Andrews KY16 8LB, UK

<sup>3</sup> Department of Chemistry, University of York, York, UK

<sup>4</sup> Department of Physics, University of York, York, UK

<sup>5</sup> SUERC, University of Glasgow, Glasgow, UK

<sup>6</sup> Department of Marine and Environmental Sciences, Savannah State University, Savannah, GA, USA

<sup>7</sup> Department of Electrical and Computer Engineering, George Mason University, Fairfax, VA, USA

<sup>8</sup> Present Address: School of Ocean and Earth Science, University of Southampton, Southampton SO14 3ZH, UK

<sup>9</sup> Present Address: Department of Mechanical & Aerospace Engineering, State University of New York at Buffalo, Buffalo, NY, USA

**Keywords** Biomineral · Ocean acidification · Raman · Organic matrix

## Introduction

Coral reefs support high biodiversity (Knowlton et al. 2010) and provide a range of ecosystem services (Moberg and Folke 1999; Woodhead et al. 2019), so it is important to understand how coral biomineralisation will respond to expected future environmental change. Coral skeletons are composite materials of aragonite and biomolecules (e.g. lipids, proteins, polysaccharides) which are embedded within the aragonite crystallites (Cuif et al. 1997, 2005; Dauphin et al. 2006; Drake et al. 2020). The skeleton can form from an amorphous CaCO<sub>3</sub> (ACC) precursor produced intracellularly in the layer of epidermal coral cells adjacent to the skeleton (Mass et al. 2017; Sun et al. 2020). In addition, skeletal growth may occur by direct attachment of Ca<sup>2+</sup>

and  $\text{CO}_3^{2-}$  ions epitaxially to the crystallites in the existing skeleton at an extracellular calcification site, sandwiched between the skeleton and the base of the polyp, which is at least, partly isolated from seawater (Sun et al. 2020).

The skeletal biomolecules are produced by the coral holobiont (Falini et al. 2015) and synthesised by the coral calcicoblastic cells, the bottom tissue layer at the base of the organism (Puverel et al. 2007). The organic matrix contains proteins which can be rich in acidic amino acids (aspartic acid and glutamic acid) and which have  $\text{Ca}^{2+}$  binding properties (Puverel et al. 2005). This organic matrix is inferred to exert control over the biomineralisation process as biomolecules affect  $\text{CaCO}_3$  nucleation (Picker et al. 2012),  $\text{CaCO}_3$  polymorph (Falini et al. 2013), precipitation rate (Kellock et al. 2020, 2022), crystal morphology (Tong et al. 2004; Reggi et al. 2016) and material properties (Kim et al. 2016).

Increased seawater  $\text{pCO}_2$  can influence coral skeleton morphology by increasing or reducing calyx size (Tambutté et al. 2015; Allison et al. 2022, respectively), by increasing or reducing the coenosteum area which connects adjacent corallites (Allison et al. 2022; Scucchia et al. 2021, respectively) or by altering the corallite morphology (Scucchia et al. 2021; Allison et al. 2022). It is unclear how these morphological changes are mediated, but some observations are suggestive. The organic content (Coronado et al. 2019), protein content (Tambutté et al. 2015) and amino acid content (Kellock et al. 2020) of skeletons are increased in tropical corals cultured at high seawater  $\text{pCO}_2$  (an ocean acidification scenario).

Massive *Porites* spp. corals are an important reef building coral species in the Indo-Pacific Ocean (Veron 1993). The most prevalent amino acid in the *Porites* spp. coral skeletal organic matrix is aspartic acid (Cuif et al. 1999; Kellock et al. 2020). This biomolecule inhibits aragonite precipitation at the aspartic acid concentrations estimated at the coral calcification site (Kellock et al. 2020), and the extent of inhibition is affected by the seawater saturation state ( $\Omega_{\text{aragonite}}$ ). Observations of fluorescent dyes at the external coral calcification site indicate that the pH of the calcification media is elevated above that of seawater (Venn et al. 2011, 2013, 2019) and decreases at high seawater  $\text{pCO}_2$  (Venn et al. 2013, 2019, 2022). This likely results in a reduction in calcification media  $\Omega_{\text{aragonite}}$  which could affect the influence of the biomolecules at the calcification site.

The present study explores the effects of seawater  $\text{pCO}_2$  and temperature on the amino acid composition and aragonite lattice disorder of massive *Porites* spp. skeletons. We analyse the skeletal amino acids of a suite of corals cultured at 25 °C and 28 °C and at seawater  $\text{pCO}_2$  of 180, 400 and 750  $\mu\text{atm}$  (Cole et al. 2018), respectively, representing approximate  $\text{CO}_2$  concentrations under glacial, early twenty-first century and projected future conditions (Gattuso and Lavigne 2009). Prior to culturing, the corals were collected

from a reef in Fiji where seasonal seawater temperatures typically range from ~26 to 29 °C (Wu et al. 2013) and the upper temperature during culturing is likely to be below the thermal stress threshold for these specimens. We use Raman spectroscopy to analyse the coral skeletons and additional specimens cultured at the same temperatures but at seawater  $\text{pCO}_2$  260  $\mu\text{atm}$  (representing pre-industrial  $\text{CO}_2$  concentrations) and an additional set of massive *Porites* spp. corals cultured at varying seawater  $\text{pCO}_2$  and analysed previously for skeletal amino acids (Kellock et al. 2020). Raman spectroscopy has been used to identify the  $\text{CaCO}_3$  polymorph (Nehrke and Nouet 2011), to explore  $\text{CO}_3$  disorder in the  $\text{CaCO}_3$  lattice (Nehrke and Nouet 2011; Kamenos et al. 2013; DeCarlo et al. 2017), map the distribution of skeletal organic material (Nehrke and Nouet 2011; DeCarlo et al. 2018) and infer Mg content in biogenic carbonate (Kamenos et al. 2013; DeCarlo et al. 2017). We compare the organic contents and  $\text{CO}_3$  disorder in the different coral skeletons to identify how seawater  $\text{pCO}_2$  and temperature influence these aspects of the coral biomineralisation process. We also analyse the Raman spectra of a suite of synthetic aragonite precipitated over variable temperature and  $\Omega$  to identify how these parameters influence disorder in a similar but non-biological system. We compare these to the spectra from the coral samples to yield insights into the environmental factors controlling coral skeleton Raman signature.

## Methods

### Coral samples

#### Coral culturing

Full details of the coral culturing are provided in Cole et al. (2018) and the supplementary material. In this research, we study the skeletons of massive *Porites* spp. corals cultured over seawater  $\text{pCO}_2$  and temperature by Cole et al. (2018) (reported as experiment 2). In brief, 4 individual coral heads (defined as separate genotypes on the basis that they were collected from spatially separate colonies) were imported into the UK. Each head was divided into sub-colonies (~12 cm in diameter) and at least one piece of each was cultured at 28 °C and ~180, 260, 400 and 750 seawater  $\text{pCO}_2$ . Seawater  $\text{pCO}_2$  was gradually adjusted over a 1-month period and then corals were maintained at these conditions for 4 months and then stained with alizarin red S to create a marker in the skeleton. Calcification (along with photosynthesis and respiration) of each sub-colony was measured 3–4 times over the next 5 weeks (the experimental period) while the corals were maintained at constant conditions. Thereafter the corals were stained again and the seawater temperature was reduced to 25 °C over 4 weeks. The corals were

acclimated at this temperature for 4 weeks, stained again and then physiological rates were measured over another 5-week experimental period. Physiological rates are reported in Cole et al. (2018).

At the end of the study the corals were sacrificed, and the skeletons cleaned by submergence in 3–4% sodium hypochlorite for  $\geq 24$  h with intermittent agitation. The skeletons were rinsed and dried and sawn into slices. The skeleton deposited within each of the 25 and 28 °C experimental periods was sampled from the maximum growth axis using a microdrill with a bit of diameter 100  $\mu\text{m}$ . The skeleton was crushed to a powder with an agate mortar and pestle. Aliquots of the drilled coral powders were analysed for amino acid content and Raman analysis. Seawater [ $\text{PO}_4^{3-}$ ] in the first week of the 5-week experimental period in the 400  $\mu\text{atm}$   $\text{pCO}_2$  treatment at 28 °C was below the limit of detection (0.00  $\mu\text{M}$ , Cole et al. 2021) and lower than observed in typical reef sites (Szmant 2002). The culture seawater for this treatment was discarded and replaced with seawater sourced from the remaining 3 reservoirs bubbled to bring it to seawater  $\text{pCO}_2$  of 400  $\mu\text{atm}$  before use. The geochemistry of these specimens was therefore only analysed in the skeleton deposited at 25 °C.

#### Amino acid analysis

Amino acid analysis was conducted on the skeletons of 3 of the 4 coral genotypes (termed G4, G6 and G7 in Cole et al. (2018)) and in individuals cultured at 180, 400 and 750  $\mu\text{atm}$  at 25 °C and at 180 and 750  $\mu\text{atm}$  at 28 °C following the method of Tomiak et al. 2013. Skeletal samples were subject to an extensive cleaning programme to remove any remnants of the coral tissue and endolithic organisms, e.g. algae (Le Campion-Alsumard et al. 1995), and to leave only intra-crystalline material.

All reagents are analytical grade unless otherwise reported. In brief, < 20 mg of powdered skeletal sample (< 100  $\mu\text{m}$ ) was accurately weighed into a plastic microcentrifuge tube and bleached using 50  $\mu\text{L}$  12%  $\text{NaOCl}$   $\text{mg}^{-1}$  for 48 h, followed by the removal of the bleach and sequential rinsing with 18.2  $\text{M}\Omega$   $\text{H}_2\text{O}$  and methanol. Samples were dried overnight. To hydrolyse the peptide bonds in the samples, < 10 mg was accurately weighed into a 2-mL sterile glass vial (Wheaton) and 20  $\mu\text{L}$   $\text{mg}^{-1}$  7 M  $\text{HCl}$  was added. After a flush with nitrogen, the vials were heated at 110 °C for 24 h. Upon removal, samples were dried in a centrifugal evaporator overnight. Samples were rehydrated and analysed using reverse-phase HPLC with fluorescence detection, following a modified method of Kaufman and Manley (1998). This enables quantification of L and D isomers of 12 amino acids. As asparagine and glutamine undergo deamination during the preparation process, they will contribute to observed concentrations of aspartic acid and glutamic

acid. However, proteomics suggests that the contributions of asparagine and glutamine to coral skeletal proteins are small. For example, 56 aspartic acid and 5 asparagine residues occur in an acidic amino acid-rich protein (CARP3) isolated from a coral skeleton (Mass et al. 2013). Similarly, 24 glutamic acid and 1 glutamine residues occur in the same protein (Mass et al. 2013).

We report aspartic acid/asparagine as Asx and glutamic acid/glutamine as Glx. Other amino acids are abbreviated as follows: serine (Ser), L-threonine (L-Thr), glycine (Gly), L-arginine (L-Arg), alanine (Ala), valine (Val), phenylalanine (Phe), leucine (Leu) and isoleucine (Ile). All samples were run in duplicate alongside standards and blanks. Analyses of replicate drilled coral powders ( $n=5$ ) indicate that the standard deviation ( $1\sigma$ ) of repeat analyses is  $\pm 125$ , 34, 51 and 13  $\text{pmol mg}^{-1}$  for total amino acid, Asx, Gly and Glx, respectively, equivalent to coefficients of variation of 8%, 4%, 20% and 7%, respectively (Kellock et al 2020). For the remaining amino acids, standard deviation ( $1\sigma$ ) of [amino acid] of replicate analyses was always < 12  $\text{pmol mg}^{-1}$ . The contribution of each amino acid to the total amino acid was calculated as [amino acid]/[total amino acid], with both quantities in  $\text{pmol mg}^{-1}$ . Inclusion of the stain did not affect the mol% of different amino acid groups (Kellock et al. 2020).

#### Raman spectroscopy

Raman spectroscopy was used to analyse all the coral skeletons cultured at 25 °C (4 coral genotypes: G4, G5, G6 and G7  $\times 4$   $\text{pCO}_2$  treatments), those cultured at 180, 260 and 750  $\mu\text{atm}$  at 28 °C and all the synthetic aragonite precipitates. Raman spectra were also collected on 11 additional *Porites* spp. skeletons, cultured in our laboratory at 25 °C and 180, 400 and 750  $\mu\text{atm}$  seawater  $\text{pCO}_2$  (Cole et al. 2018 reported as experiment 1 with coral genotypes defined as G1, G2 and G3). Two sub-colonies of coral genotype G3 were cultured at 400 and 750  $\mu\text{atm}$ . These are defined as replicates 1 and 2 in each case.

Raman spectra were collected with a Renishaw In-Via Qontor Raman Microscope using a NIR 300 mW 785 nm solid state laser. Spectra were collected in static mode from 100 to 1311  $\text{cm}^{-1}$  with the laser set at 5% full power with a 1200  $\text{cm}^{-1}$  grating and a spectral resolution of  $\sim 0.3$   $\text{cm}^{-1}$ . The laser spot was focused onto a particle of sample powder and data were collected for 2 s for each acquisition. 10 acquisitions were repeated on each spot and summed to yield the final spectrum. Twelve to fifteen spots were analysed on each sample powder. All the Raman spectra had lattice mode peaks at  $\sim 153$  and 206  $\text{cm}^{-1}$  (DeCarlo et al. 2018) and a doublet  $\nu_4$  peak (Urmos et al. 1991), indicative of aragonite. The spectra were processed using OriginLabs peak processing software and the peak centre and the full width half

maxima (FWHM) of the  $\nu_1$  peak were estimated following a Voigt fit (Meier 2005). This  $\nu_1$  band results from symmetric C–O stretching in the planar carbonate group (Bischoff et al. 1985) and broadening of this peak is indicative of increased local disorder around the  $\text{CO}_3^{2-}$  group. Measured FWHM were corrected to true FWHM using the instrument spectral resolution (Nasdala et al. 2001).

We analysed a milled synthetic aragonite powder as an in-house reference material at frequent intervals during each day of Raman analyses. This aragonite was precipitated at  $\text{pH}_{\text{NBS}}$  8.445 and  $\Omega = 11$  and ground in an agate ball mill with water. The peak centre of this reference material drifted by  $> 0.7 \text{ cm}^{-1}$  over the first 2 h of the session (Fig. S1a) but the FWHM of the peak was stable (Fig. S1b). After this 2-h drift period, the peak centre population was normally distributed (Shapiro–Wilk test for normality,  $p = 0.68$ ,  $n = 50$ ). The FWHM population of this reference material was normally distributed over the entire session ( $p = 0.98$ ,  $n = 100$ ).

Particle size can influence Raman spectroscopy (Gómez et al. 2019). To test the effect of particle size on the FWHM of the aragonite  $\nu_1$  peak, we compared the Raman spectra of the milled aragonite particles with that of the same aragonite sample before milling. The aragonite particles produced during the laboratory precipitation had approximate diameters of  $\sim 70$ – $120 \mu\text{m}$  (Fig. S2a) while the milled aragonite had dimensions of  $\sim 3$ – $5 \mu\text{m}$  (Fig. S2b). We collected Raman spectra of both the ground and unground aragonite particles and found that  $\nu_1$  FWHM in the ground aragonite ( $4.52 \pm 0.07$ , 1 s,  $n = 14$ ) was not significantly different from that of the unground aragonite ( $4.54 \pm 0.06$ , 1 s,  $n = 13$ ) as tested by  $t$  test for equal means ( $p = 0.37$ ). The coral skeletal samples measured by Raman had dimensions within the range represented by the milled and unmilled reference material so we do not consider particle size influences FWHM in this study.

Corals were stained with alizarin red S while living to create temporal markers in the skeleton (see Cole et al. 2021 for images of a stained skeleton). To test if the stain influenced the Raman spectrum, we drilled a coral skeleton powder along a stain line and compared it to the skeleton deposited immediately underneath the stain. The mean FWHM of the  $\nu_1$  peak in the stained skeleton ( $\text{FWHM} = 4.08 \pm 0.10 \text{ cm}^{-1}$ , 1 s,  $n = 12$ ) was not significantly different from that of the unstained skeleton ( $\text{FWHM} = 4.06 \pm 0.09 \text{ cm}^{-1}$ , 1 s,  $n = 15$ ) as tested by  $t$  test for equal means ( $p = 0.55$ ).

Preliminary spectra of the same powders were collected using a 532-nm laser with an 1800 grating in extended mode from  $102$ – $3202 \text{ cm}^{-1}$  in an attempt to use the Raman instrument to identify variations in the fluorescence associated with skeletal organic matrix between skeletons (DeCarlo et al. 2018). These preliminary analyses demonstrate that fluorescence (mean signal intensity at  $2400$ – $2700 \text{ cm}^{-1}$  normalised to the  $\nu_1$  peak) is about  $3 \times$  higher in the stained

skeleton compared to the unstained skeleton (Fig. S3a). Furthermore, C–H bonding peaks are not visible in the Raman spectra in either the stained or unstained skeleton (Fig. S3b). Due to the high signal from the alizarin red S stain, we did not undertake further analyses of these samples using the 532-nm laser.

### Synthetic aragonite

To investigate the effects of  $\Omega$  and temperature on the peak centre and FWHM of the aragonite Raman spectrum  $\nu_1$  peak, we analysed synthetic aragonite precipitated over varying  $\Omega$  and temperature using a Metrohm Titrando 902 titrator (Castillo Alvarez et al. 2024). We precipitated the aragonite from seawater in the laboratory using a pH stat titrator which dosed  $\text{Na}_2\text{CO}_3$  and  $\text{CaCl}_2$  solutions to replace the ions removed during aragonite formation. To explore the effect of  $\Omega$ , aragonite was precipitated at  $\text{pH}_{\text{NBS}}$  8.545,  $T = 25 \text{ }^\circ\text{C}$  and  $\Omega = 4, 7, 10, 13$  and  $18$ . To explore the effect of temperature, aragonite was precipitated at  $\Omega = 14$  and  $T = 10, 15, 20, 25$  and  $30 \text{ }^\circ\text{C}$ . Measurements of the  $[\text{CO}_3^{2-}]$  and pH of the extracellular calcification media in corals suggest the media has a  $\Omega_{\text{aragonite}}$  of about  $12$  (Sevilgen et al. 2019).

## Results

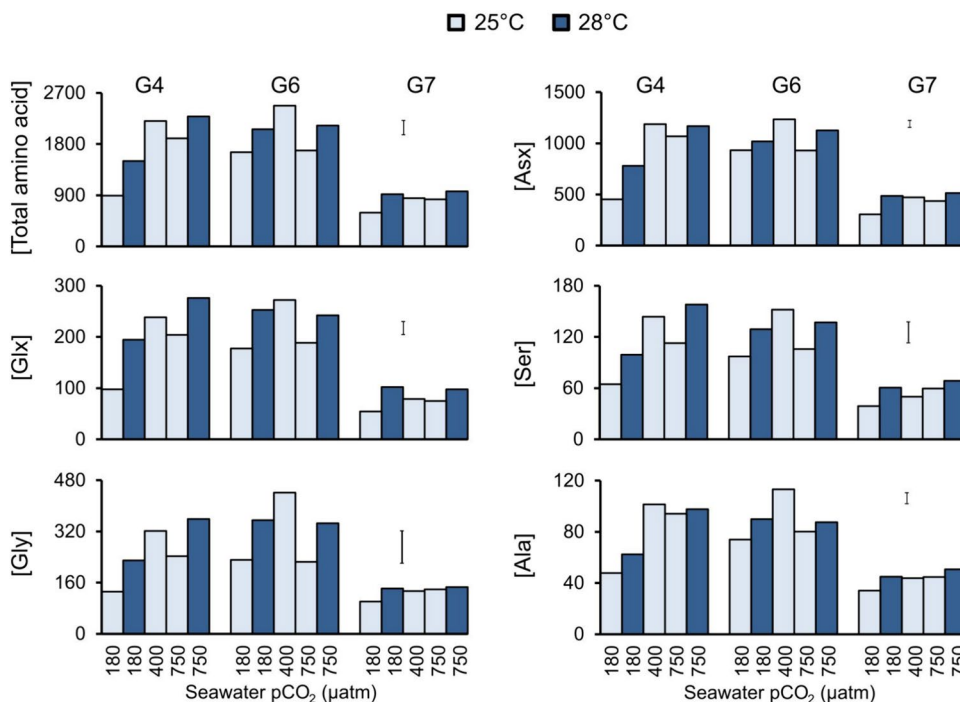
The supplementary information contains all data for skeletal amino acid concentrations (Table S1), Raman data of coral skeletons and synthetic aragonites (Tables S2 and S3, respectively).

### Amino acids in cultured coral skeletons

Asx is the most common amino acid in the coral skeletons, typically making up about half of the total amino acid content (Fig. 1). Glx, Gly and Ser typically make up  $\sim 11, 15$  and  $6\%$ , respectively, of the total skeletal amino acid (Fig. 1). Histidine is rarely detected in the coral skeletons and we removed this amino acid from the analysis. Skeletal [amino acid] differs considerably between different coral genotypes cultured at the same conditions (Fig. 1).

We used a paired  $t$  test to test for variations in the amino acid concentrations between temperature treatments. For this test we matched the [amino acid] in the  $25 \text{ }^\circ\text{C}$  and  $28 \text{ }^\circ\text{C}$  regions of each skeleton (same genotype and same seawater  $\text{pCO}_2$ ) and pooled all the seawater  $\text{pCO}_2$  treatments. For example, we pair the total amino acid concentration for coral genotype 4 at  $25 \text{ }^\circ\text{C}$  and  $180 \mu\text{atm}$  with the total amino acid concentration for coral genotype 4 at  $28 \text{ }^\circ\text{C}$  and  $180 \mu\text{atm}$ . We create similar pairs for all the corals skeletons and then test for variations in skeletal [amino acid] at  $25 \text{ }^\circ\text{C}$  and  $28 \text{ }^\circ\text{C}$ . Similarly, to test for the influence of seawater  $\text{pCO}_2$

**Fig. 1** Concentrations of total and key amino acids (p mol mg<sup>-1</sup>) in the skeletons of the 3 coral genotypes (G4, G6 and G7) cultured over varying seawater pCO<sub>2</sub> and temperature. Typical standard deviations of repeat analysis of replicates of skeletal powders are shown by error bars (Kellock et al. 2020)



on skeletal composition, we matched the [amino acid] in the skeleton of each genotype cultured at 25 °C or 28 °C with that of the same genotype cultured at the same temperature but different pCO<sub>2</sub> and used paired *t* tests to test for difference in [amino acid] between pCO<sub>2</sub> treatments; for example, we pair the total amino acid concentration for coral genotype 4 at 25 °C and 180 μatm with the total amino acid concentration for coral genotype 4 at 25 °C and 750 μatm and the total amino acid concentration for coral genotype 4 at 28 °C and 180 μatm with the total amino acid concentration for coral genotype 4 at 28 °C and 750 μatm, etc.

[Asx], [Glx], [Gly], [Ser] and [total amino acids] are significantly lower at 25 °C compared to 28 °C, over all seawater pCO<sub>2</sub> treatments (Table 1; Fig. 1). [Asx], [Glx], [Gly], [Ser], [Ala], [L-Thr] and [total amino acids] are significantly lower at 180 μatm compared to 400 μatm. [Ser] is also significantly reduced at 180 μatm compared to 750 μatm, but otherwise skeletal amino acid concentrations do not vary significantly between pCO<sub>2</sub> treatments (Table 1).

To test if the contribution of each amino acid to the total amino acid content of the skeleton is influenced by temperature or seawater pCO<sub>2</sub>, we calculate the molar proportions of

**Table 1** *p* values of paired *t* tests to test for differences in [amino acid] between seawater pCO<sub>2</sub> and temperature treatments

Amino acid	Seawater pCO <sub>2</sub> (μ atm)			Temperature
	180 vs. 400	400 vs. 750	180 vs. 750	25 °C vs. 28 °C
[Asx]	<b>0.021 (180 &lt; 400)</b>	0.19	0.084	<b>0.039 (25 °C &lt; 28 °C)</b>
[Glx]	<b>0.042 (180 &lt; 400)</b>	0.35	0.15	<b>0.0073 (25 °C &lt; 28 °C)</b>
[Gly]	<b>0.027 (180 &lt; 400)</b>	0.22	0.14	<b>0.038 (25 °C &lt; 28 °C)</b>
[Ser]	<b>0.015 (180 &lt; 400)</b>	0.35	<b>0.040 (180 &lt; 750)</b>	<b>0.0069 (25 °C &lt; 28 °C)</b>
[Ala]	<b>0.0056 (180 &lt; 400)</b>	0.17	0.084	0.055
[Leu]	0.20	0.40	0.46	0.83
[Val]	0.062	0.25	0.25	0.11
[L-Thr]	<b>0.045 (180 &lt; 400)</b>	0.42	0.075	0.096
[Arg]	0.13	0.50	0.38	0.29
[Ile]	0.18	0.25	0.63	0.57
[Phe]	0.11	0.27	0.32	0.47
[Total amino acid]	<b>0.014 (180 &lt; 400)</b>	0.19	0.092	<b>0.010 (25 °C &lt; 28 °C)</b>

Significant results (*p* ≤ 0.05) are highlighted in bold and the direction of difference is summarised in parentheses

each amino acid in the skeleton as [amino acid]/[total amino acid] with both quantities in  $\text{pmol mg}^{-1}$ . We use paired  $t$  tests to test for differences between temperature and seawater  $\text{pCO}_2$  treatments as before. Variations in the relative contributions of the amino acid to total amino acid are almost always insignificant (Table 2), with the exception that the contribution of Glx to total amino acid is significantly higher at 28 °C compared to 25 °C, while the contribution of Ala to total amino acid is significantly lower at the higher temperature (Fig. 2).

### Skeletal amino acids, coral calcification rate and calcification media pH

To further explore controls on skeletal amino acids, we conduct multiple linear regression analyses modelling the skeletal amino acid concentrations as a function of coral calcification rate and coral calcification media pH. For this exercise the data from the present study are combined with skeletal amino acid data from a previous experiment, in which *Porites* spp. were cultured at 25 °C in our laboratory (Kellock et al. 2020). Calcification rates from the current study and the previous experiment are already published as

experiment 2 and experiment 1, respectively, in Cole et al. (2018). Coral calcification media pH are derived from skeletal  $\delta^{11}\text{B}$  measurements of the same coral skeletons (Allison et al. 2018, 2021 for experiments 1 and 2, respectively). Calcification is significantly related to all detected skeletal amino acids and total amino acids but calcification media pH is not (Table 3).

We use one-way ANCOVA tests to compare linear relationships between calcification rate and skeletal concentration of each amino acid at 25 °C and 28 °C (Table 3). We observe no significant differences in the relationships between calcification rate and concentrations of skeletal amino acids at the 2 temperatures, with the exception that [Glx] is offset to a higher concentration at comparable calcification rates at 28 °C compared to 25 °C (Fig. 3). These relationships are also illustrated for Asx and Ala in Fig. 3.

### Raman spectroscopy of coral skeletons

FWHM values for the carbonate  $\nu_1$  Raman mode of the coral skeletons are shown in Fig. 4. To test the influence of seawater temperature on FWHM, we use a paired  $t$  test matching the FWHM of each individual coral at 25 °C

**Table 2**  $p$  values of paired  $t$  tests to test for differences in the proportional contribution of each amino acid to total amino acids between seawater  $\text{pCO}_2$  and temperature treatments

[Amino acid]/[total amino acid]	Seawater $\text{pCO}_2$ ( $\mu\text{atm}$ )			Temperature
	180 vs 400	400 vs 750	180 vs 750	25 °C vs 28 °C
[Asx]	0.40	0.82	0.22	0.66
[Glx]	0.15	0.37	0.12	<b>0.0069 (25 °C &lt; 28 °C)</b>
[Gly]	0.95	0.57	0.11	0.62
[Ser]	0.16	0.17	0.68	0.49
[Ala]	0.70	0.68	0.76	<b>0.021 (25 °C &gt; 28 °C)</b>
[Leu]	0.51	0.95	0.31	0.24
[Val]	0.20	0.77	0.12	0.33
[L-Thr]	0.38	0.23	0.95	0.33
[Arg]	0.21	0.66	0.18	0.53
[Ile]	0.32	0.60	0.060	0.22
[Phe]	0.25	0.89	0.12	0.15

Significant results ( $p \leq 0.05$ ) are highlighted in bold and the direction of difference is summarised in parentheses

**Fig. 2** Changes in the molar contribution of **a** Glx and **b** Ala to the total skeletal amino acids as a function of  $\text{pCO}_2$  and temperature. Contributions are calculated as [amino acid]/[total], with both amounts in  $\text{pmol mg}^{-1}$ . Typical standard deviations of repeat analysis of replicates of skeletal powders are shown by error bars (Kellock et al. 2020)

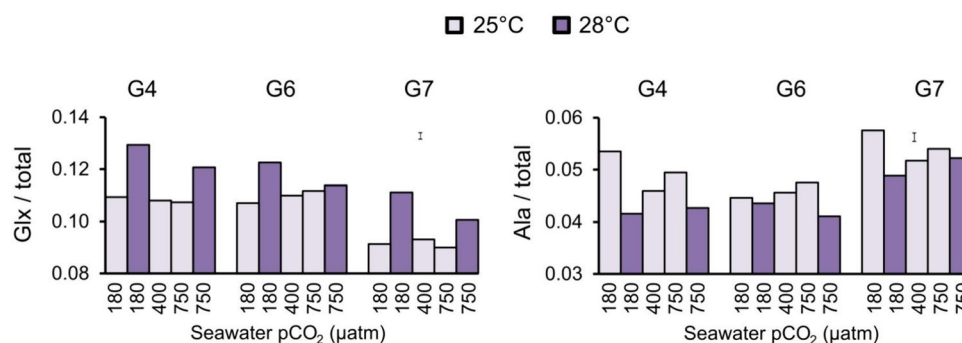


**Table 3**  $p$  values of multiple regression analysis models to predict concentrations of each coral skeletal amino acid from coral calcification rate and calcification media pH ( $\text{pH}_{\text{CM}}$ ) and ANCOVA  $p$  values to compare linear relationships between calcification rate and [amino acid] at 25 °C and 28 °C.  $p$  values  $\leq 0.05$  are highlighted in bold

Amino acid	Multiple linear regression $p$ value to predict skeletal amino acid		ANCOVA $p$ value to compare regressions at 25 and 28 °C	
	$\text{pH}_{\text{CM}}$	Calcification rate	Equal means	Equal slopes
[Asx]	<b>0.91</b>	$8.7 \times 10^{-5}$	0.10	0.39
[Glx]	<b>0.67</b>	$4.0 \times 10^{-4}$	<b>0.0053</b>	0.83
[Gly]	<b>0.64</b>	$2.4 \times 10^{-2}$	0.35	0.99
[Ser]	<b>0.93</b>	$3.7 \times 10^{-4}$	0.077	0.71
[Ala]	<b>0.90</b>	$2.4 \times 10^{-4}$	0.41	0.49
[Leu]	<b>0.43</b>	$6.7 \times 10^{-3}$	0.50	0.70
[Val]	<b>0.47</b>	$1.3 \times 10^{-3}$	0.19	0.87
[L-Thr]	<b>0.79</b>	$2.4 \times 10^{-3}$	0.27	0.71
[Arg]	<b>0.30</b>	$2.7 \times 10^{-3}$	0.10	0.67
[Ile]	<b>0.41</b>	$7.5 \times 10^{-3}$	0.47	0.82
[Phe]	<b>0.52</b>	$6.7 \times 10^{-3}$	0.42	0.72
[Total amino acid]	<b>0.83</b>	$3.9 \times 10^{-4}$		

and 28 °C for each  $\text{pCO}_2$  treatment. At 28 °C the FWHM are significantly narrower than at 25 °C ( $p = 0.015$ ). To test for variations in FWHM between  $\text{pCO}_2$  treatments, we pool all coral genotypes and test the effect of  $\text{pCO}_2$  at each temperature separately by one-way ANOVA. We observe no significant effect of seawater  $\text{pCO}_2$  on FWHM at 25 °C or 28 °C ( $p = 0.469$  and  $0.324$ , respectively).

Further we determine the FWHM of the  $\nu_1$  peak for each coral as a function of coral calcification rate,  $\text{pH}_{\text{CM}}$  and skeletal Asx (the most common amino acid in the

skeleton, Fig. 5). None of these parameters is significant related to FWHM at 25 °C or 28 °C (Table 4).

### Raman spectroscopy of synthetic aragonite

We observe positive relationships between Raman aragonite spectra FWHM and both  $\Omega_{\text{aragonite}}$  and water temperature in the synthetic aragonite precipitates (Fig. 6a, b). Temperature and  $\Omega_{\text{aragonite}}$  are positively related to aragonite precipitation rate in these experiments (Castillo Alvarez et al. 2024) and we plot aragonite FWHM as a function of precipitation rate for experiments conducted at variable  $\Omega_{\text{aragonite}}$  and at 25 °C or at variable temperature and  $\Omega_{\text{aragonite}} = 14$  (Fig. 6c). One-way ANCOVA indicates that relationships between aragonite precipitation rate and FWHM do not vary significantly between the 2 datasets ( $p$  equal means = 0.38,  $p$  equal slopes = 0.96).

### Discussion

#### Environmental change and coral skeletal amino acids

Asx, Glx and Gly are the most common skeletal amino acids as reported previously in *Porites* spp. and many other corals (Cuif et al. 1999; Puvarel et al. 2005). In the present study, skeletal [Asx], [Glx], [Gly], [Ser] and [total amino acids] are significantly lower at 25 °C compared to 28 °C but the contribution of Asx, Gly and Ser to total skeletal amino acid is not altered significantly by temperature (Fig. 1; Table 1). Calcification increases by 66% on average at 28 °C compared to 25 °C in the 3 coral genotypes analysed in the present study (Cole et al. 2018) although we note that the effect of temperature on calcification rate is seawater  $\text{pCO}_2$  dependent (Cole et al. 2018). However, calcification rate is significantly inversely related to all detected skeletal amino

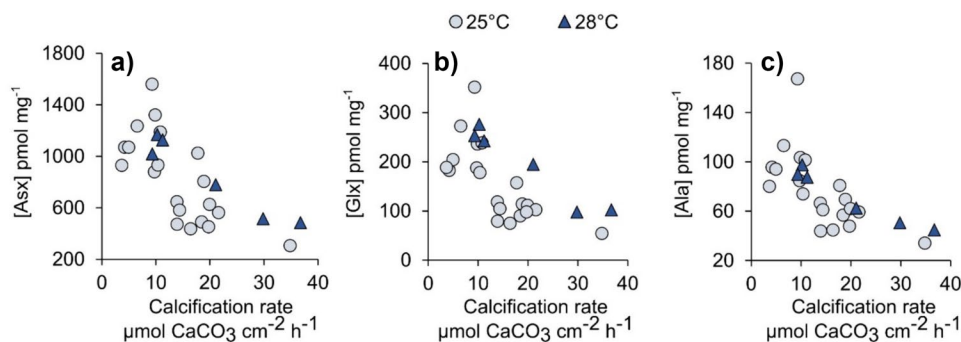


**Fig. 3** Relationships between skeletal **a** [Asx], **b** [Glx] and **c** [Ala] and calcification rate in corals cultured at 25 and 28 °C. At 25 °C, skeletal amino acid from this study is combined with data from a previous experiment in which *Porites* spp. were cultured at 25 °C in our

laboratory (Kellock et al. 2020). Corals from all  $\text{pCO}_2$  treatments are pooled for this analysis. All calcification data are reported in Cole et al. (2018)

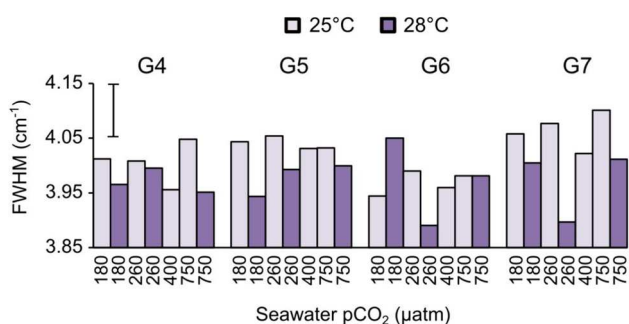
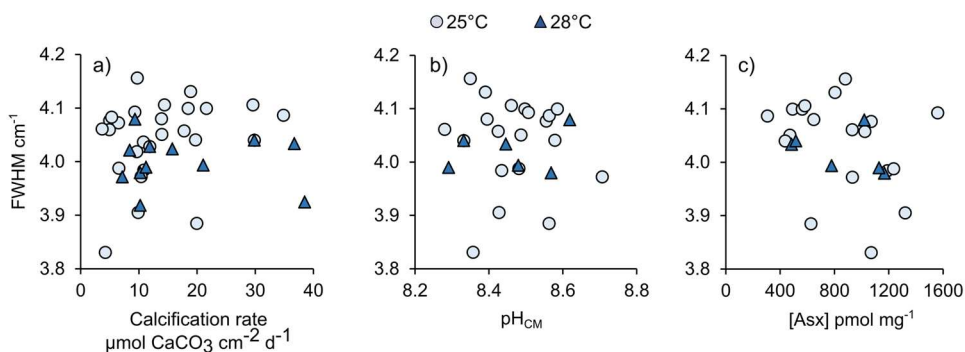


**Fig. 4** FWHM of the  $\nu_1$  peak in the aragonite Raman spectrum of the corals cultured at various pCO<sub>2</sub> and temperature. The typical standard deviation of multiple analyses ( $n=12$  to  $15$ ) of a single sample is shown

acids and total amino acids (Table 3, illustrated for Asx, Glx and Ala in Fig. 3). Although this seems counterintuitive (given that skeletal [amino acids] increase at high temperature when calcification is usually higher), the inverse relationship between skeletal [amino acid] and calcification reflects the large variation in calcification rate between the coral genotypes. For example, genotype G7 contains low concentrations of skeletal [amino acid] (Fig. 1) but has high calcification rates compared to genotype G6, which has a lower calcification rate but higher skeletal [amino acid] (Supplementary data, Table 1). These data show that skeletal [amino acid] is significantly higher in skeletons from corals with relatively low calcification rates.

Our observation that skeletal [amino acid] usually increases at higher temperature when calcification rate also increases (on average), indicates that the skeletal [amino acid] does not reflect dilution of the biomolecules by the CaCO<sub>3</sub> produced each day, i.e. resulting in high skeletal [amino acid] at low calcification rates (as hypothesised by Kellock et al. 2020). Rather, higher amounts of skeletal protein must be produced at higher temperatures. Although more skeleton is also precipitated at these higher temperatures, the mass of protein incorporated into the skeleton, as a function of skeletal mass, still increases.

**Fig. 5** The FWHM of the Raman spectrum  $\nu_1$  peak for each coral as a function of **a** coral calcification rate ( $\mu\text{mol CaCO}_3 \text{ cm}^{-2} \text{ d}^{-1}$ ), **b** pH<sub>CM</sub> (total scale) and **c** skeletal [Asx]



Temperature does not affect the relative contribution of each amino acid to [total amino acid], with the exception that the proportion of Glx is lower at 25 °C compared to 28 °C, while the proportional contribution of Ala to total amino acid is higher at the low temperature (Table 2). These changes reflect alterations in the protein compositions of the skeletal organic matrix deposited at the 2 temperatures. Many studies on the proteomic responses of corals to temperature focus on the effects of heat stress (e.g. Mayfield et al. 2018; Stuhr et al. 2018), rather than on temperature increases below the stress threshold such as tested here (Cole et al. 2018). However, several studies indicate that the concentration and composition of coral tissue biomolecules is temperature dependent. For example, seasonal temperature variations altered the genomic response of *Acropora millepora* (Wuitchik et al. 2019), and temperature significantly influenced the physiological profile of *Porites* spp. corals living along an environmental gradient (McLachlan et al. 2021), including affecting tissue biomass and soluble protein and lipid content. Seasonal variations in coral tissue lipid content were positively correlated with seawater temperature in *Goniastera aspera* (Oku et al. 2003) and temperature significantly affected the tissue lipid compositions of the coral analysed in the present study (von Xylander et al. 2023).

The amino acids for coral protein synthesis can be sourced from seawater, from heterotrophy or are synthesised by the coral or by the algal symbionts (Grover et al.

**Table 4** Coefficients of determination ( $r^2$ ) and  $p$  values for relationships between Raman aragonite spectra  $\nu_1$  peak FWHM and coral parameters. All pCO<sub>2</sub> treatments are pooled for this analysis

	25 °C		28 °C	
	$r^2$	$p$	$r^2$	$p$
Calcification rate	0.06	0.24 ( $n=27$ )	0.00	0.83 ( $n=12$ )
pH <sub>CM</sub>	0.00	0.78 ( $n=20$ )	0.08	0.59 ( $n=6$ )
[Asx]	0.09	0.21 ( $n=20$ )	0.13	0.48 ( $n=6$ )
[Total amino acids]	0.04	0.43 ( $n=20$ )	0.09	0.55 ( $n=6$ )
Multiple linear regression (all)	0.27	0.28 ( $n=20$ )	0.98	0.22 ( $n=6$ )

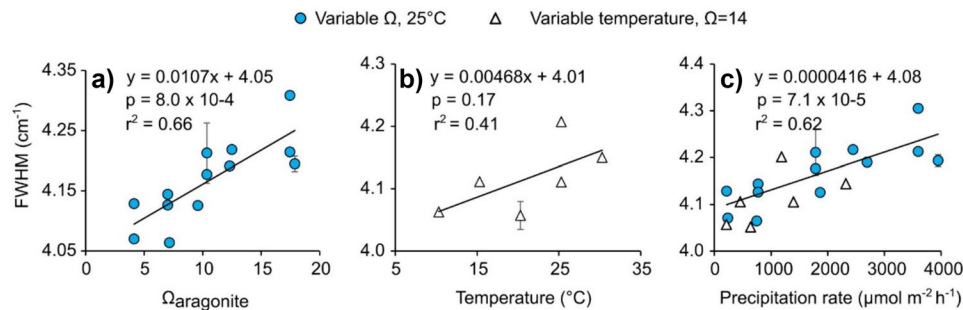


**Fig. 6** FWHM of the  $\nu_1$  peak in the aragonite Raman spectrum of the synthetic aragonite precipitates cultured over variable **a**  $\Omega$  and **b** temperature. In **c** data from experiments at variable  $\Omega$  and temperature are combined onto one graph as a function of aragonite precipitation

rate. The typical standard deviation of multiple analyses ( $n = 12$  to  $15$ ) of a single sample is shown. Lines indicate best fit linear relationships and  $p$  values and coefficients of variations are shown. In **c** the line fits the entire dataset (experiments over a range of  $\Omega$  and temperature)

2008; Ferrier-Pagès et al. 2021). Glutamic acid, glutamine, aspartic acid, and Ala are probably synthesised both by *Porites australiensis* and its symbionts (Shinzato et al. 2014). However, glutamic acid and Ala (along with Ser and Thr) compositions varied significantly between the skeletons of symbiont-bearing and non-symbiotic corals, such that glutamic acid is relatively enriched and Ala depleted in the skeletons of symbiotic corals (Cuif et al. 1999). This disparity may indicate that glutamic acid is predominantly sourced from the symbionts and Ala from the host. In support of this, glutamate in the sea anemone *Aiptasia pulchella* (a close coral relative) is predominantly synthesised in the symbionts (Swanson and Hoegh-Guldberg 1998). In the present study, the shift to higher skeletal [Glx] at higher temperatures (Fig. 2) may indicate an increased contribution of symbiont amino acids to the host amino acid pool, although we note that both net and gross photosynthesis are lower at 28 °C compared to 25 °C in these corals (Cole et al. 2018).

There are significant inverse relationships between coral calcification rate and skeletal [amino acid] in all the amino acids tested with the exception of His (Table 3). It is unclear if the skeletal organic matrix acts to promote or inhibit the formation of the aragonite mineral. The morphology and polymorph of  $\text{CaCO}_3$  precipitated in vitro is influenced by the presence of the organic matrix extracted from coral skeletons (Falini et al. 2013). Aspartic acid, glutamic acid and Gly suppress aragonite precipitation at  $\geq 0.2$  mM at the approximate pH and dissolved inorganic carbon conditions of the coral calcification site (Kellock et al. 2020, 2022; Castillo Alvarez et al. 2024), although lower concentrations of aspartic acid (1–10  $\mu\text{M}$ ) may promote aragonite formation to a minor degree (Kellock et al. 2022). The influence of amino acids on calcite precipitation is affected by peptide chain length (Elhadj et al. 2006) and further work is required to clarify how coral skeletal proteins (rather than their amino acid constituents) affects aragonite formation.

With respect to seawater  $\text{pCO}_2$ , skeletal concentrations of Asx, Glx, Gly, Ser, Ala, L-Thr and total amino acid are lower at 180  $\mu\text{atm}$  compared to 400  $\mu\text{atm}$ , but otherwise the only difference between seawater  $\text{pCO}_2$  treatments is that [Ser] is reduced at 180  $\mu\text{atm}$  compared to 750  $\mu\text{atm}$ . Concentrations of skeletal, Asx, Glx, Ala and total amino acids were positively correlated with seawater  $\text{pCO}_2$  in a previous study (Kellock et al. 2020). Skeletal [amino acid] varies by more than  $\times 2$  between different coral genotypes cultured under the same environmental conditions in the present study (Fig. 1) and in another experiment in our aquarium (Kellock et al. 2020). This large variation between coral genotypes, combined with our small sample size, makes it difficult to resolve an influence of seawater  $\text{pCO}_2$  on skeletal amino acids.

### Raman spectroscopy of coral aragonite $\text{CO}_3$ disorder

The decrease in coral skeleton aragonite Raman spectra  $\nu_1$  peak FWHM between corals cultured at 28 °C compared to 25 °C is small ( $0.05 \text{ cm}^{-1}$ , on average), but statistically significant. The smaller FWHM reflects an increase in local order around the  $\text{CO}_3$  group with higher temperature. We examine the Raman spectra of synthetic aragonites precipitated over variable  $\Omega$  and temperature (Castillo Alvarez et al. 2024) to explore the influence of these parameters on aragonite  $\text{CO}_3$  group disorder. However, we note that these abiogenic precipitations do not fully encompass the conditions of the coral calcification media which contains complex biomolecules and enzymes (Tambutté et al. 2011).

#### *The response of aragonite $\text{CO}_3$ disorder to $\Omega$ and temperature in synthetic aragonite*

The Raman analyses of the synthetic aragonite precipitates demonstrates that the FWHM of the aragonite  $\nu_1$  peak is significantly positively related to  $\Omega_{\text{aragonite}}$  of the precipitating seawater (Fig. 6a). The FWHM is also positively related to

temperature ( $r^2 = 0.41$ ) but this relationship is not significant due to the small number of precipitates ( $n = 6$ ). Both temperature and  $\Omega$  influence aragonite precipitation rate (Castillo Alvarez et al. 2024) and we observe no significant difference in the precipitation rate versus FWHM relationship between experiments conducted over variable temperature or  $\Omega$  (Fig. 6c). This suggests that aragonite precipitation rate influences the FWHM rather than  $\Omega_{\text{aragonite}}$  or temperature. The origin of this effect is unclear, but rotational disorder of the  $\text{CO}_3$  group may reflect disturbance of the aragonite lattice to accommodate trace elements (DeCarlo et al. 2017; Farfan et al. 2022) in place of the mineral host ions ( $\text{Ca}^{2+}$  and  $\text{CO}_3^{2-}$ ). If mineral precipitation rates are rapid, then these impurity ions are more likely to be entrapped in the mineral (the growth entrapment model, Watson 2004), thus increasing disorder.

Our observation that  $\Omega$  influences FWHM agrees with DeCarlo et al. (2017), although the magnitude of the effect is far smaller in the present study. DeCarlo et al. (2017) reported a logarithmic relationship between solution  $\Omega$  and FWHM equivalent to an increase in FWHM of  $\sim 0.05 \text{ cm}^{-1}/\Omega$  from  $\Omega = 10$  to 15 and  $0.04 \text{ cm}^{-1}/\Omega$  from  $\Omega = 15$  to 20. This is considerably higher than observed in the present study ( $0.011 \text{ cm}^{-1}/\Omega$ ). The  $\text{Ca}^{2+}$  consumed from the seawater during aragonite formation was not replaced during the titrations in the DeCarlo et al. (2017) study, leading to large variations in solution  $[\text{Ca}^{2+}]$  and  $\Omega$  within each precipitation ( $> 70\%$ , Holcomb et al 2016). This  $[\text{Ca}^{2+}]$  drop almost certainly affects aragonite precipitation rate. Further work is required to determine how this variability influences FWHM.

#### Causes of coral aragonite $\text{CO}_3$ disorder

Although aragonite precipitation rate influences FWHM in synthetic aragonite (Fig. 6), we do not observe significant relationships between coral calcification rate and FWHM in the skeletal samples (Fig. 5, Table 4). Calcification rates are highly variable between different coral genotypes and  $\text{pCO}_2$  treatments (Cole et al. 2018) but, for the 4 coral genotypes cultured here at both temperatures, calcification increases by 39%, on average, at the higher temperature. This temperature increase is associated with a narrowing of the Raman  $\nu_1$  FWHM, which is contrary to our observation that higher temperatures increase the FWHM in synthetic aragonite. We hypothesise that the increase of Raman  $\nu_1$  FWHM in synthetic aragonite precipitates at high precipitation rates reflects an increased uptake of trace elements at a rapidly advancing crystal surface (Section “The response of aragonite  $\text{CO}_3$  disorder to  $\Omega$  and temperature in synthetic aragonite”). However, high calcification rates in tropical corals do not necessarily reflect fast rates of crystal growth. Corals extend their skeletons along a growth axis, but the

crystal fibres which make up the bulk of the skeleton are not orientated parallel to this axis (Wells 1956) so rapid skeletal extension does not necessarily equate with rapid fibre growth. Rapid coral calcification rates may reflect extension of many fibres, rather than rapid extension of individual fibres.

We do not observe significant relationships between skeletal Raman  $\nu_1$  FWHM and coral calcification media pH,  $[\text{Asx}]$  or  $[\text{total amino acid}]$  (Fig. 5, Table 4). To identify the potential origin of the change in coral skeletal Raman  $\nu_1$  FWHM, we summarise the observed influences of temperature,  $\Omega_{\text{aragonite}}$  and  $[\text{aspartic acid}]$  on the FWHM of synthetic aragonite in Fig. 7. Increasing seawater temperature by  $3^\circ\text{C}$  increases the FWHM in synthetic aragonite by  $0.014 \text{ cm}^{-1}$  (Fig. 6b) and, as already noted, this cannot explain the observed decrease in coral skeletal FWHM at higher temperature. Skeletal  $[\text{Asx}]$  and other amino acids are higher in corals cultured at  $28^\circ\text{C}$  compared to  $25^\circ\text{C}$  (Table 1).  $[\text{Asx}]$  can be highly variable between coral genotypes, but comparing the skeletal  $[\text{Asx}]$  for each coral specimen cultured at both  $25$  and  $28^\circ\text{C}$  indicates that skeletal  $[\text{Asx}]$  increases by 23% on average at the higher temperature. Increasing seawater  $[\text{aspartic acid}]$  increases the Raman  $\nu_1$  FWHM of synthetic aragonite (Kellock et al. 2022), but the effect is small, such that a 23% increase in seawater aspartic acid increases aragonite FWHM by  $\sim 0.006 \text{ cm}^{-1}$  (shown in Fig. 7). It is unclear how biomolecules are incorporated into aragonite and coral skeletons. Coral skeletons are composed of nanograins (typically tens of nm in dimension) which are enveloped within materials inferred to be organic (Cuif et al. 2004; Drake et al. 2020; Tan et al. 2023). This suggests the skeleton is a nanocomposite composed of 2 materials intimately related at the nanoscale. However, inclusion of biomolecules within the aragonite structure cannot be discounted. In coral skeletons, Asx predominantly occurs in proteins rather

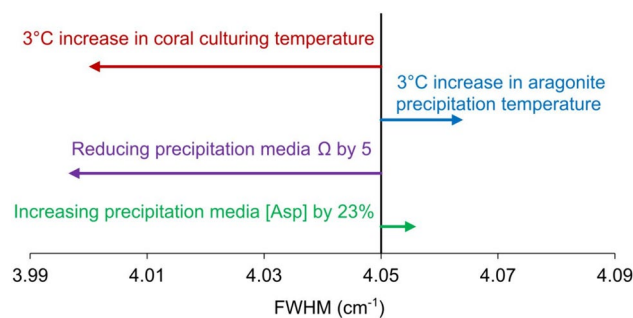


**Fig. 7** A comparison of the effect of a  $3^\circ\text{C}$  increase in coral culturing temperature on the FWHM of the  $\nu_1$  peak in the coral skeleton Raman spectrum with the influences of precipitation media temperature and  $\Omega$  and  $[\text{aspartic acid}]$  in synthetic aragonite. Temperature and  $\Omega$  influences are estimated from Fig. 6 (this study). The effect of aspartic acid is calculated from Kellock et al. 2022 which observed a linear relationship between aragonite  $\nu_1$  peak FWHM and seawater  $\log[\text{aspartic acid}]$  above  $[\text{aspartic acid}] = 10 \mu\text{M}$

than as the free amino acids used in the synthetic aragonite experiments (Kellock et al. 2022), however.

These latter experiments suggest that the increase in skeletal amino acid at higher temperature is not responsible for the observed decrease in skeletal FWHM.

The decrease in skeletal  $\nu_1$  peak FWHM at higher temperature could reflect a decrease in calcification media  $\Omega$  (Fig. 6a), as hypothesised by DeCarlo et al. (2017). Comparisons of the effect of temperature increases on coral calcification and synthetic aragonite precipitation rate suggests that coral calcification media  $\Omega$  decreases from 25 to 28 °C at low seawater  $p\text{CO}_2$  (180 and 260  $\mu\text{atm}$ ), but increases at 750  $\mu\text{atm}$  seawater  $p\text{CO}_2$  (Cole et al. 2018; Allison et al. 2021). Coral skeletal boron geochemistry (B/Ca and  $\delta^{11}\text{B}$ ) suggests that the effects of temperature on coral calcification media pH and  $\Omega_{\text{aragonite}}$  are complicated. Calcification media pH was significantly lower in massive *Porites* spp. cultured at 28 °C compared to 25 °C at low (180  $\mu\text{atm}$ ) but not at high (750  $\mu\text{atm}$ ) seawater  $p\text{CO}_2$  (Allison et al. 2021) and was unaffected by temperature in a range of coral species cultured at ~300–3300  $\mu\text{atm}$  seawater  $p\text{CO}_2$  (Eagle et al. 2022). However, reduced temperatures were associated with lower calcification media pH at high  $p\text{CO}_2$  in cultured *Porites* spp. (Comeau et al. 2019) but with higher calcification media pH in corals spanning a range of localities in Western Australia (Ross et al. 2019) and in a long term (1939–2013) coral record from the Great Barrier Reef (D’Olivo et al. 2019). Similarly, boron geochemistry estimates of  $\Omega_{\text{aragonite}}$  may decrease at higher temperature in cultured corals (Eagle et al. 2022) but are either unrelated or positively related to temperature in tropical corals growing along a temperature gradient on reefs (Ross et al. 2019). A recent study found an offset between estimates of coral calcification media pH measured directly by the pH sensitive dye SNARF and inferred from skeletal  $\delta^{11}\text{B}$  (Allison et al. 2023), suggesting that other processes besides pH may influence skeletal  $\delta^{11}\text{B}$ . This will affect estimates of coral calcification media  $\Omega$  from boron geochemistry. Our synthetic aragonite observations (Fig. 6) suggest a decrease in  $\Omega_{\text{aragonite}}$  of > 5 is required to generate the small decrease in FWHM observed in the corals cultured at 28 °C in this study. This is large in comparison with the observed decrease in calcification media  $\Omega$  reported by Eagle et al. 2022 where  $\Omega$  decreased by 1.1 on average in response to a 3 °C temperature increase. Further work is required to resolve the response of coral calcification media  $\Omega$  to temperature change and to identify if this influences coral aragonite structural disorder.

## Conclusions

This study shows that some skeletal [amino acids] of *Porites* spp. corals, grown in laboratory culture, are increased by

rises in seawater temperature below the thermal stress threshold. Biomolecules control the polymorph, morphology and precipitation rate of calcareous minerals (Wolf et al. 2007; Kellock et al. 2020; Kim et al. 2016). In addition, the inclusion of amino acids within  $\text{CaCO}_3$  (calcite) improves the material hardness (Kim et al. 2016) and biomolecules are inferred to contribute to the superior material properties of  $\text{CaCO}_3$  biominerals compared to their abiogenic analogues (Deng et al. 2022). However, Raman spectroscopy indicates that disorder around the  $\text{CO}_3$  in the aragonite lattice of the coral skeletons is reduced at higher temperatures. This is contrary to observations in synthetic aragonite where increases in the temperature and [amino acid] of the precipitating media both increase  $\text{CO}_3$  disorder. Understanding the effect of biomolecules on aragonite structure and material properties is in its infancy, and future work will resolve if changes in skeletal protein content are likely to alter the physical resilience of coral skeletons.

**Acknowledgements** This work was supported by the Leverhulme Trust (Research project Grant 2015-268 to NA, RK, and KP) and the UK Natural Environment Research Council (NE/G015791/1 to NA and AAF; NE/S001417/1 to NA, KP, RK, MC and AAF). We thank David Miller and Aaron Naden, University of St Andrews, for assistance with Raman analyses. The Raman microscope at the University of St. Andrews is supported by the EPSRC Light Element Analysis Facility Grant EP/T019298/1 and the EPSRC Strategic Equipment Resource Grant EP/R023751/1.

**Funding** Natural Environment Research Council, NE/S001417/1, Nicola Allison, NE/G015791/1, Adrian A. Finch, Leverhulme Trust, 2015-268, Nicola Allison.

## Declarations

**Conflict of interest** On behalf of all authors, the corresponding author states that there is no conflict of interest.

**Open Access** This article is licensed under a Creative Commons Attribution 4.0 International License, which permits use, sharing, adaptation, distribution and reproduction in any medium or format, as long as you give appropriate credit to the original author(s) and the source, provide a link to the Creative Commons licence, and indicate if changes were made. The images or other third party material in this article are included in the article’s Creative Commons licence, unless indicated otherwise in a credit line to the material. If material is not included in the article’s Creative Commons licence and your intended use is not permitted by statutory regulation or exceeds the permitted use, you will need to obtain permission directly from the copyright holder. To view a copy of this licence, visit <http://creativecommons.org/licenses/by/4.0/>.

## References

- Allison N, Cole C, Hintz C, Hintz K, Rae J, Finch AA (2018) The effect of ocean acidification on tropical coral calcification: insights from calcification fluid DIC chemistry. *Chem Geol* 497:162–169

- Allison N, Cole C, Hintz C, Hintz K, Rae J, Finch A (2021) Resolving the interactions of ocean acidification and temperature on coral calcification media pH. *Coral Reefs* 40(6):1807–1818
- Allison N, Ross P, Brasier A, Cieminska N, Lopez Martin N, Cole C, Hintz C, Hintz K, Finch A (2022) Effects of seawater pCO<sub>2</sub> on the skeletal morphology of massive *Porites* spp. corals. *Mar Biol* 169(6):73
- Allison N, Venn AA, Tambutté S, Tambutté E, Wilckens FK, Kasemann SA, Craven J, Talavera C, de Hoog C (2023) A comparison of SNARF-1 and skeletal  $\delta^{11}\text{B}$  estimates of calcification media pH in tropical coral. *Geochim Cosmochim Acta* 355:184–194
- Bischoff WD, Sharma SK, MacKenzie FT (1985) Carbonate ion disorder in synthetic and biogenic magnesian calcites: a Raman spectral study. *Am Miner* 70(5–6):581–589
- Castillo Alvarez MC, Penkman K, Kröger R, Finch AA, Clog M, Brasier A, Still J, Allison N (2024) Insights into the response of coral biomineralisation to environmental change from aragonite precipitations in vitro. *Geochim Cosmochim Acta* 364:184–194
- Cole C, Finch AA, Hintz C, Hintz K, Allison N (2018) Effects of seawater pCO<sub>2</sub> and temperature on calcification and productivity in the coral genus *Porites* spp.: an exploration of potential interaction mechanisms. *Coral Reefs* 37:471–481
- Cole C, Finch AA, Hintz C, Hintz K, Yu Y, Allison N (2021) The KD Sr/Ca in cultured massive *Porites* spp. corals are reduced at low seawater pCO<sub>2</sub>. *Geochim Cosmochim Acta* 314:55–67
- Comeau S, Cornwall CE, DeCarlo TM, Doo SS, Carpenter RC, McCulloch MT (2019) Resistance to ocean acidification in coral reef taxa is not gained by acclimatization. *Nature Clim Chang* 9:477–483
- Coronado I, Fine M, Bosellini FR, Stolarski J (2019) Impact of ocean acidification on crystallographic vital effect of the coral skeleton. *Nat Commun* 10:1–9
- Cuif JP, Dauphin Y, Gautret P (1997) Biomineralization features in scleractinian coral skeletons: source of new taxonomic criteria. *Boletin De La Real Sociedad Espanola De Historia Nat (seccion Geologica)* 92:129–141
- Cuif JP, Dauphin Y, Freiwald A, Gautret P, Zibrowius H (1999) Biochemical markers of zooxanthellae symbiosis in soluble matrices of skeleton of 24 *Scleractinia* species. *Comp Biochem Physiol—A Mol Integr Physiol* 12:269–278
- Cuif JP, Dauphin Y, Berthet P, Jegoudez J (2004) Associated water and organic compounds in coral skeletons: quantitative thermogravimetry coupled to infrared absorption spectrometry. *Geochem Geophys Geosyst*. <https://doi.org/10.1029/2004GC000783>
- Dauphin Y, Cuif JP, Massard P (2006) Persistent organic components in heated coral aragonitic skeletons—implications for palaeoenvironmental reconstructions. *Chem Geol* 231(1–2):26–37
- DeCarlo TM, D’Olivo JP, Foster T, Holcomb M, Becker T, McCulloch MT (2017) Coral calcifying fluid aragonite saturation states derived from Raman spectroscopy. *Biogeosciences* 14(22):5253–5269
- DeCarlo TM, Ren H, Farfan GA (2018) The origin and role of organic matrix in coral calcification: insights from comparing coral skeleton and abiogenic aragonite. *Front Mar Sci* 5:170
- Deng Z, Jia Z, Li L (2022) Biomineralized materials as model systems for structural composites: intracrystalline structural features and their strengthening and toughening mechanisms. *Adv Sci* 9(14):2103524
- D’Olivo JP, Ellwood G, DeCarlo TM, McCulloch MT (2019) Deconvolving the long-term impacts of ocean acidification and warming on coral biomineralisation. *Earth Planet Sci Lett* 526:115785
- Drake JL, Mass T, Stolarski J, Von Euw S, van de Schootbrugge B, Falkowski PG (2020) How corals made rocks through the ages. *Glob Change Biol* 26(1):31–53
- Eagle RA, Guillermic M, De Corte I, Alvarez Caraveo B, Bove CB, Misra S, Cameron LP, Castillo KD, Ries JB (2022) Physicochemical control of caribbean coral calcification linked to host and symbiont responses to varying pCO<sub>2</sub> and Temperature. *J Marine Sci Eng* 10(8):1075
- Elhadj S, Salter EA, Wierzbicki A, De Yoreo JJ, Han N, Dove PM (2006) Peptide controls on calcite mineralization: polyaspartate chain length affects growth kinetics and acts as a stereochemical switch on morphology. *Cryst Growth Des* 6(1):197–201
- Falini G, Reggi M, Fermani S, Sparla F, Goffredo S, Dubinsky Z, Levi O, Dauphin Y, Cuif JP (2013) Control of aragonite deposition in colonial corals by intra-skeletal macromolecules. *J Struct Biol* 183(2):226–238
- Falini G, Fermani S, Goffredo S (2015) Coral biomineralization: a focus on intra-skeletal organic matrix and calcification. *Semin Cell Dev Biol* 46:17–26
- Farfan GA, Apprill A, Cohen A, DeCarlo TM, Post JE, Waller RG, Hansel CM (2022) Crystallographic and chemical signatures in coral skeletal aragonite. *Coral Reefs* 41(1):19–34
- Ferrier-Pagès C, Martinez S, Grover R, Cybulski J, Shemesh E, Tchernov D (2021) Tracing the trophic plasticity of the coral–dino-flagellate symbiosis using amino acid compound-specific stable isotope analysis. *Microorganisms* 9(1):182
- Gattuso JP, Lavigne H (2009) Approaches and software tools to investigate the impact of ocean acidification. *Biogeosciences* 6(10):2121–2133
- Gómez DA, Coello J, Maspoeh S (2019) The influence of particle size on the intensity and reproducibility of Raman spectra of compacted samples. *Vib Spectrosc* 100:48–56
- Grover R, Maguer JF, Allemant D, Ferrier-Pagès C (2008) Uptake of dissolved free amino acids by the scleractinian coral *Stylophora pistillata*. *J Exp Biol* 211(6):860–865
- Holcomb M, DeCarlo TM, Gaetani GA, McCulloch M (2016) Factors affecting B/Ca ratios in synthetic aragonite. *Chem Geol* 437:67–76
- Kamenos NA, Burdett HL, Aloisio E, Findlay HS, Martin S, Longbone C, Dunn J, Widdicombe S, Calosi P (2013) Coralline algal structure is more sensitive to rate, rather than the magnitude, of ocean acidification. *Glob Change Biol* 19(12):3621–3628
- Kaufman DS, Manley WF (1998) A new procedure for determining DL amino acid ratios in fossils using reverse phase liquid chromatography. *Quat Sci Rev* 17:987–1000
- Kellock C, Cole C, Penkman K, Evans D, Kröger R, Hintz C, Hintz K, Finch A, Allison N (2020) The role of aspartic acid in reducing coral calcification under ocean acidification conditions. *Sci Rep* 10(1):12797
- Kellock C, Castillo Alvarez MC, Finch A, Penkman K, Kröger R, Clog M, Allison N (2022) Optimising a method for aragonite precipitation in simulated biogenic calcification media. *PLoS ONE* 17(12):e0278627
- Kim YY, Carloni JD, Demarchi B, Sparks D, Reid DG, Kunitake ME, Tang CC, Duer MJ, Freeman CL, Pokroy B, Penkman K, Meldrum F (2016) Tuning hardness in calcite by incorporation of amino acids. *Nat Mater* 15(8):903–910
- Knowlton N, Brainard RE, Fisher R, Moews M, Plaisance L, Caley MJ, (2010) Coral reef biodiversity. In: *Life in the world’s oceans: diversity distribution and abundance*, pp. 65–74
- Le Champion-Alsumard T, Golubic S, Hutchings P (1995) Microbial endoliths in skeletons of live and dead corals: *Porites lobata* (Moorea, French Polynesia). *Marine Ecology Prog Ser* 117:149–157
- Mass T, Drake JL, Haramaty L, Kim JD, Zelzion E, Bhattacharya D, Falkowski PG (2013) Cloning and characterization of four novel coral acid-rich proteins that precipitate carbonates in vitro. *Curr Biol* 23(12):1126–1131
- Mass T, Giuffrè AJ, Sun CY, Stiffler CA, Frazier MJ, Neder M, Tamura N, Stan CV, Marcus MA, Gilbert PU (2017) Amorphous

- calcium carbonate particles form coral skeletons. *Proc Natl Acad Sci USA* 114:E7670–E7678
- Mayfield AB, Chen YJ, Lu CY, Chen CS (2018) The proteomic response of the reef coral *Pocillopora acuta* to experimentally elevated temperatures. *PLoS ONE* 13(1):e0192001
- McLachlan RH, Price JT, Muñoz-García A, Weisleder NL, Jury CP, Toonen RJ, Grottoli AG (2021) Environmental gradients drive physiological variation in Hawaiian corals. *Coral Reefs* 40(5):1505–1523
- Meier RJ (2005) On art and science in curve-fitting vibrational spectra. *Vib Spectrosc* 2(39):266–269
- Moberg F, Folke C (1999) Ecological goods and services of coral reef ecosystems. *Ecol Econ* 29(2):215–233
- Nasdala L, Banerjee A, Hager T, Hofmeister W, (2001) Laser Raman microspectroscopy in mineralogical research. *Microscopy and Analysis*, pp.11–14
- Nehrke G, Nouet J (2011) Confocal Raman microscope mapping as a tool to describe different mineral and organic phases at high spatial resolution within marine biogenic carbonates: case study on *Nerita undata* (Gastropoda, Neritopsina). *Biogeosciences* 8(12):3761–3769
- Oku H, Yamashiro H, Onaga K, Sakai K, Iwasaki H (2003) Seasonal changes in the content and composition of lipids in the coral *Goniastrea aspera*. *Coral Reefs* 22:83–85
- Picker A, Kellermeier M, Seto J, Gebauer D, Cölfen H (2012) The multiple effects of amino acids on the early stages of calcium carbonate crystallization. *Zeitschrift für Krist* 227:744–757
- Puverel S, Tambutté E, Pereira-Mouries L, Zoccola D, Allemand D, Tambutté S (2005) Soluble organic matrix of two Scleractinian corals: partial and comparative analysis. *Comp Biochem Physiol B: Biochem Mol Biol* 141(4):480–487
- Puverel S et al (2007) Evidence of low molecular weight components in the organic matrix of the reef building coral, *Stylophora pistillata*. *Comp Biochem Physiol—A Mol Integr Physiol* 147:850–856
- Reggi M et al (2016) Influence of intra-skeletal coral lipids on calcium carbonate precipitation. *CrystEngComm* 18:8829–8833
- Ross CL, DeCarlo TM, McCulloch MT (2019) Environmental and physiochemical controls on coral calcification along a latitudinal temperature gradient in Western Australia. *Glob Change Biol* 25(2):431–447
- Scucchia F, Malik A, Zaslansky P, Putnam HM, Mass T (2021) Combined responses of primary coral polyps and their algal endosymbionts to decreasing seawater pH. *Proc R Soc B* 288(1953):20210328
- Sevilgen DS, Venn AA, Hu MY, Tambutté E, de Beer D, Planas-Bielsa V, Tambutté S (2019) Full in vivo characterization of carbonate chemistry at the site of calcification in corals. *Sci Adv*. <https://doi.org/10.1126/sciadv.aau744>
- Shinzato C, Inoue M, Kusakabe M (2014) A snapshot of a coral “holobiont”: a transcriptome assembly of the scleractinian coral, *Porites*, captures a wide variety of genes from both the host and symbiotic zooxanthellae. *PLoS ONE* 9(1):e85182
- Stuhr M, Blank-Landeshammer B, Reymond CE, Kollipara L, Sickmann A, Kucera M, Westphal H (2018) Disentangling thermal stress responses in a reef-calcifier and its photosymbionts by shotgun proteomics. *Sci Rep* 8(1):3524
- Sun CY, Stiffler CA, Chopdekar RV, Schmidt CA, Parida G, Schoeppler, Fordyce BI, Brau JH, Mass T, Tambutté S, Gilbert PU (2020) From particle attachment to space-filling coral skeletons. *Proc Natl Acad Sci USA* 117:30159–30170
- Swanson R, Hoegh-Guldberg O (1998) Amino acid synthesis in the symbiotic sea anemone *Aiptasia pulchella*. *Mar Biol* 131:83–93
- Szmant AM (2002) Nutrient enrichment on coral reefs: is it a major cause of coral reef decline? *Estuaries* 25:743–766
- Tambutté S, Holcomb M, Ferrier-Pagès C, Reynaud S, Tambutté É, Zoccola D, Allemand D (2011) Coral biomineralization: from the gene to the environment. *J Exp Mar Biol Ecol* 408(1–2):58–78
- Tambutté E, Venn AA, Holcomb M, Segonds N, Techer N, Zoccola D, Allemand D, Tambutté S (2015) Morphological plasticity of the coral skeleton under CO<sub>2</sub>-driven seawater acidification. *Nature Commun* 6(1):7368
- Tan CD, Hähner G, Fitzer S, Cole C, Finch AA, Hintz C, Hintz K, Allison N (2023) The response of coral skeletal nano structure and hardness to ocean acidification conditions. *Royal Soc Open Sci* 10(8):230248
- Tomiak PJ et al (2013) Testing the limitations of artificial protein degradation kinetics using known-age massive *Porites* coral skeletons. *Quat Geochronol* 16:87–109
- Tong H et al (2004) Control over the crystal phase, shape, size and aggregation of calcium carbonate via a L-aspartic acid inducing process. *Biomaterials* 25:3923–3929
- Urmos J, Sharma SK, Mackenzie FT (1991) Characterization of some biogenic carbonates with Raman spectroscopy. *Am Miner* 76(3–4):641–646
- Venn AA, Tambutté E, Holcomb M, Allemand D, Tambutté S (2011) Live tissue imaging shows reef corals elevate pH under their calcifying tissue relative to seawater. *PLoS ONE* 6:e20013
- Venn AA, Tambutté E, Holcomb M, Laurent J, Allemand D, Tambutté S (2013) Impact of seawater acidification on pH at the tissue-skeleton interface and calcification in reef corals. *Proc Natl Acad Sci USA* 110:1634–1639
- Venn AA, Tambutté E, Caminiti-Segonds N, Techer N, Allemand D, Tambutté S (2019) Effects of light and darkness on pH regulation in three coral species exposed to seawater acidification. *Sci Rep* 9:1–12
- Venn AA, Tambutté E, Comeau S, Tambutté S (2022) Proton gradients across the coral calcifying cell layer: effects of light, ocean acidification and carbonate chemistry. *Front Mar Sci* 9:973908
- Veron JEN (1993) Corals of Australia and the Indo-pacific. University of Hawaii Press, Honolulu
- Von Xylander NS, Young SA, Cole C, Smith TK, Allison N (2023) Sterols, free fatty acids, and total fatty acid content in the massive *Porites* spp. corals cultured under different pCO<sub>2</sub> and temperature treatments. *Coral Reefs* 42(2):551–566
- Watson E (2004) A conceptual model for near-surface kinetic controls on the trace-element and stable isotope composition of abiogenic calcite crystals. *Geochim Cosmochim Acta* 68:1473–1488
- Wells JW (1956) Scleractinia. In: Moore RC (ed) Treatise on invertebrate paleontology, Part F, Coelenterata. University of Kansas Press, Lawrence, pp 328–444
- Wolf SE, Loges N, Mathiasch B, Panthöfer M, Mey I, Janshoff A, Tremel W (2007) Phase selection of calcium carbonate through the chirality of adsorbed amino acids. *Angew Chem Int Ed* 46(29):5618–5623
- Woodhead AJ, Hicks CC, Norström AV, Williams GJ, Graham NA (2019) Coral reef ecosystem services in the Anthropocene. *Funct Ecol* 33(6):1023–1034
- Wu HC, Linsley BK, Dassié EP, Schiraldi B, deMenocal PB (2013) Oceanographic variability in the South Pacific Convergence Zone region over the last 210 years from multi-site coral Sr/Ca records. *Geochem Geophys Geosyst* 14:1435–1453. <https://doi.org/10.1029/2012GC004293>
- Wuitchik DM, Wang DZ, Pells TJ, Karimi K, Ward S, Vize PD (2019) Seasonal temperature, the lunar cycle and diurnal rhythms interact in a combinatorial manner to modulate genomic responses to the environment in a reef-building coral. *Mol Ecol* 28(16):3629–3641